PRESYNAPTIC MUSCARINIC-NICOTINIC MODULATION of GABAergic INPUTS to NEURONS in the REM SLEEP (REM-S) EXECUTIVE AREA of the ROSTRAL PONS

Esteban Pino[1, 2, *], Héctor Kunizawa[1] and Michel Borde[1, *]

1- Laboratorio de Neurofisiología Celular y Sináptica, Unidad Académica de Fisiología, Facultad de Medicina. Gral. Flores 2125. 11800 Montevideo, URUGUAY.

2- Present address: Department of Neurobiology and Animal Physiology, Neurophysiology, University of Regensburg. Universitätsstraße 31, 93040, Regensburg, Germany.

*** Corresponding authors: Michel Borde**

Email: mborde@fmed.edu.uy

ORCID: 0000-0002-5729-8616

Esteban Pino

Email: esteban.pino@biologie.uni-regensburg.de

Key words: REM sleep, ultradian, behavioral states, pontine reticular formation, PnO, Acetylcholine, GABA, Muscarine, Nicotine, presynaptic plasticity.

Running title: Cholinergic modulation of GABAergic inhibition of PnO REM-on neurons.

Acknowledgements: Special thanks to Dr. Jack Yamuy without whose inspiration, creativity, work and support, this study would not have been possible. The authors like to than Drs. Ángel Núñez and Verónica Egger for helpful comments regarding the manuscript. This research was supported by FCE2009_3115-ANII, CSIC-CAP, UdelaR and PEDECIBA.

Author contribution: E.P., H.K. and M.B. conception and design of research; E.P. and H.K. performed experiments; E.P., H.K. and M.B. analyzed data and interpreted results of experiments; E.P. and H.K. prepared figures. E.P. drafted the paper and E.P. and M.B. wrote, reviewed and edited the final version of the manuscript. All authors approved its final version.

ABSTRACT

A large body of evidence indicates a pivotal role of cholinergic neurons of brainstem tegmental nuclei in the control of neurons of the reticular nucleus pontis oralis (PnO) considered executive for rapid eye movement sleep (REM-S) onset and maintenance. More recent data suggest that the PnO is also under GABAergic control that gate REM-S and highlights the role of interactions between cholinergic and GABAergic processes as a key mechanism for REM-S control. Here we employed an *in vitro* model of REM-S motor suppression to investigate the modulation of GABAergic inputs to PnO neurons by cholinergic agents. We found that carbachol, a mixed muscarinic-nicotinic cholinergic agonist, provoked either depression or facilitation of single evoked monosynaptic GABAergic IPSCs. Both effects were presynaptic in origin and likely due to the activation of different presynaptic cholinergic receptors as depression was replicated by muscarine (presynaptic inhibition) and facilitation by nicotine (presynaptic facilitation). IPSCs evoked by presumed physiological patterns of stimulation (short trains of stimuli at 15 Hz) were also affected by cholinergic agonists. Muscarine caused presynaptic inhibition accompanied by frequency facilitation and nicotine promoted the opposite effect. Notably, both agonists reduced the total inhibitory charge transferred to postsynaptic neurons during the train. Our results shed light on a possible additional mechanism for a cholinergic-mediated relief of GABAergic inhibition of PnO neurons under presumed physiological conditions, as a local component of the mutual inhibitory interaction design between sleep controlling systems at REM-s brainstem executive areas.

NEW & NOTEWORTHY

Despite decades of research into brainstem sleep mechanisms, the GABAergic-cholinergic interactions involved in gating and ultradian regulation of REM-sleep remain poorly understood. We present evidence for the functional expression of presynaptic muscarinic and nicotinic cholinergic receptors at GABAergic terminals in the pontine reticular nucleus (PnO), considered the executive area for REM-S onset and maintenance. Our results suggest that cholinergic modulation could relief reticular neurons of GABAergic inhibition. As a local component of a mutual inhibitory interaction in REM-sleep controlling systems, this interaction may help produce sharp transitions into REM sleep.

INTRODUCTION

Mesopontine neural networks are critically involved in organizing various behavioral states, such as rapid eye movement (REM) sleep and wakefulness (W) (Brown et al., 2012; Jones, 2020). A wealth of experimental evidence further supports the role of various neurotransmitters and neuromodulators in controlling the occurrence and characteristics of these states (Xi et al., 1999; 2004; Fuller et al., 2007; Luppi et al., 2006; Arrigoni et al., 2016; Scammell et al., 2017; Jones, 2020; Wang et al., 2021). Electrophysiological, pharmacological, immunohistochemical and behavioral data indicate that cholinergic and GABAergic processes converge at these pivotal mesopontine areas and interact locally to facilitate either REM-S or W. Moreover, the interplay between GABAergic and cholinergic systems may play a significant role in establishing the ultradian rhythmicity of sleep (Xi et al., 1999; 2004; Standford et al., 2003; Liang and Marks; 2009; Brown et al., 2008; Marks and Sinton, 2010; Reinoso-Suárez et al., 2010; Vanini et al., 2011). Nonetheless, the cellular and synaptic mechanisms underlying these interactions remain poorly understood.

Although the precise role of brainstem cholinergic processes in regulating REM sleep remains debated, there is broad consensus that these processes significantly contribute to its control (for reviews, see Marks & Sinton, 2010; Brown et al., 2012; Jones, 2020). Employing diverse experimental approaches -including optogenetics, pharmacogenetics, genetic manipulations for imaging and selective deletions, as well as virus-mediated circuit tracing- researchers have identified a conserved brainstem network located in the rostral pons that is critically involved in REM sleep regulation. This network comprises a distinct group of cholinergic neurons situated in the brainstem tegmental nuclei -namely, the laterodorsal (LDT) and pedunculopontine tegmental (PPT) nuclei- and their projections to glutamatergic neurons in the reticular nucleus pontis oralis (PnO), which is considered pivotal for REM sleep onset and maintenance. More recent studies have demonstrated that REM sleep–regulating circuits also include specific glutamatergic neurons within the pontine tegmentum, such as the peri-locus coeruleus α (peri-LCα) region in cats and the subcoeruleus (subLC) or sublaterodorsal nucleus (SLD) in rodents (Arrigoni et al., 2016; Saper and Fuller; 2017). Historically, cholinergic inputs to these brainstem regions were seen as essential for initiating REM sleep (Brown et al., 2012; Weber and Dan, 2016). However, more recent findings suggest that brainstem cholinergic neuronal groups primarily act as modulators rather than as the generators of REM sleep, with glutamatergic and GABAergic transmissions playing crucial roles in its timing,

generation, and maintenance (Luppi et al., 2006; Scammell et al., 2017; Niwa et al., 2018; Arrigoni & Fuller, 2019; Wang et al., 2021).

GABA has long been regarded as a sleep-promoting neurotransmitter. However, extensive research led to the incorporation of GABAergic transmission into models that explain not only the occurrence of REM-S episodes but also the sequence of different wakefulness–sleep stages (for a review see Wang et al., 2021). The primary source of GABAergic inputs to the REM sleep–executive areas in the pons has been identified as a population of neurons located in the ventrolateral periaqueductal gray (vlPAG) and the lateral pontine tegmentum (LPT) (Boissard et al., 2003; Lu et al., 2006; Sapin et al., 2009; Weber et al., 2018; Luppi et al., 2024). Additional inputs may also arise from GABAergic cells in the PnO and non-cholinergic neurons within the LDT-PPT complex (Semba, 1993; Boissard et al., 2003; Lu et al., 2006; Sapin et al., 2009; Pino et al., 2017). Seminal behavioral evidence for a GABAergic pontine mechanism controlling W and REM-S comes from experiments in unanesthetized chronic cats. These studies demonstrated that pontine microinjections of GABA or its agonists induced prolonged wakefulness, whereas administration of a GABA-A receptor antagonist resulted in long-lasting REM-S episodes (Xi et al., 1999). Subsequent rodent studies further supported a critical role for pontine GABAergic mechanisms in REM sleep control (Boissard et al., 2002; Pollock and Mistlberger, 2003; Sanford et al., 2003; Fenik and Kubin, 2009). Current evidence supports the proposal by Xi et al. (2001) that a pontine gating mechanism promotes wakefulness when the tonic activation of GABAergic neurons is high and permits REM-S when GABAergic tone is low (Sanford et al., 2003; see reviews in Arrigoni et al., 2016 and Wang et al., 2021). Furthermore, this gating mechanism likely involves a mutual inhibitory interaction between W-promoting GABAergic and REM-S-promoting cholinergic processes operating in REM-S executive brainstem areas (Xi et al., 2004; Vazquez and Baghdoyan, 2004; Fuller et al., 2007; Fenik and Kubin, 2009; Vanini et al., 2011, 2012; Weber et al., 2018).

Although postsynaptic opposing effects of GABA and cholinomimetic drugs on PnO neurons have been reported (Nuñez et al., 1997; 1998; Brown et al., 2006; Heister et al., 2009; Weng et al., 2014), most research on GABAergic and cholinergic interactions in REM-S-executive brainstem areas suggests that these interactions primarily occur at the presynaptic level. *In vivo*, the suppression of REM-S by local application of GABA at the PnO relies on the inhibition of acetylcholine (ACh) release from cholinergic terminals (Vazquez and Baghdoyan, 2004; Marks et al., 2008; Flint et al., 2010). Interestingly, in support of this model, GABA-A receptors have been identified on cholinergic varicose

axons in the PnO (Liang and Marks, 2014). In contrast, presynaptic regulation of GABAergic transmission at the PnO mediated by acetylcholine or its agonists has been less extensively investigated, and the in vitro findings remain inconclusive (Heister et al., 2009).

Based on a local, mutual inhibitory interaction between GABAergic and cholinergic processes at the PnO, we hypothesized that cholinergic inputs exert inhibitory control over GABAergic inputs to PnO neurons. To test this hypothesis, we employed an *in vitro* model of REM sleep motor suppression using rat brainstem slices (Pino et al., 2017). Our electrophysiological and pharmacological analyses provided evidence for the presence of presynaptic muscarinic (mAChRs) and nicotinic (nAChRs) acetylcholine receptors on GABAergic terminals contacting PnO neurons. We found that the activation of mAChRs and nAChRs exerts opposite effects on GABA release probability; nevertheless, both receptor activations appear to reduce the overall inhibition conveyed by GABAergic inputs during repetitive presynaptic activation. These results support the concept of a local, mutual inhibitory interaction between GABAergic and cholinergic processes in REM-S-executive brainstem areas.

MATERIALS AND METHODS

Wistar rat pups were obtained from URBE (Unidad de Reactivos Biológicos de Experimentación, School of Medicine, Universidad de la República, Uruguay). All experimental procedures adhered to ASAP/ABS Guidelines for the Use of Animals in Research and were approved by the Uruguayan Committee on Animal Research (Comisión Honoraria de Experimentación Animal, CHEA) under Protocol Number 070153-000741-15.

Mesopontine slice preparation

Mesopontine slices (~350 µm thick) containing the LDT/PPT complex, the PnO, and the trigeminal motor nucleus (MV) were obtained from 7- to 15-day-old Wistar rats using previously described methods (see Pino et al., 2017). Briefly, the animals were decapitated, a craniotomy was performed, and the brainstem was excised by transection following cerebellum removal. Throughout the procedure, the preparation was continuously bathed in modified artificial cerebrospinal fluid (ACSF) at ~4°C, containing (in mM): 213 $C_{12}H_{22}O_{11}$, 2.7 KCl, 1.25 H_2KPO_4, 2 $MgSO_4$•$7H_2O$, 26 $NaHCO_3$, 10 $C_6H_{12}O_6$, and 2 $CaCl_2$. Transverse mesopontine slices were sectioned at an inclination of approximately 4–6 degrees relative to the coronal plane using a Vibratome (Vibratome 1000plus sectioning system). Consequently, the dorsal portion of the slice was more anterior (~-8.72 mm from bregma) than the ventral aspects (~-8.30 mm; see Paxinos & Watson, 1998). Slices were stored in a holding chamber containing a 50:50 mixture of modified ACSF and standard ACSF (composition in mM: 124 NaCl, 2.7 KCl, 1.25 H_2KPO_4, 2 $MgSO_4$•$7H_2O$, 26 $NaHCO_3$, 10 $C_6H_{12}O_6$, and 2 $CaCl_2$) at room temperature (21–24°C). The ACSF pH was maintained at 7.42 by gentle bubbling with carbogen (95% O_2, 5% CO_2), and the mixture was gradually replaced (~1.5 h) with 100% standard ACSF. Slices were then transferred to a recording chamber mounted on an upright microscope stage (Nikon Eclipse FN1), equipped with infrared (IR) and differential interference contrast (DIC) imaging devices, as well as ×4 (air) and ×40 (water immersion) objectives. During recording, slices were superfused at a flow rate of ~2–3 ml/min with standard ACSF at room temperature (21–24°C).

Recording and stimulation

Whole-cell patch recordings (continuous single-electrode voltage clamp mode) were obtained from visually identified PnO neurons using IR-DIC optics. The recording area was located approximately 250 µm medial to the MV, 250 µm lateral from the midline, and 1.25 mm dorsal to the slice's ventral boundary (See Fig.1 in Pino et al., 2017). Patch pipettes (3-5 MΩ) were pulled from borosilicate glass (BF150-86-10, Sutter Instrument Co.) using a programmable puller (P-87 Sutter Instruments Co.) and filled with 'patch solution' containing (in mM): 150 KCl, 4.6 $MgCl_2$, 10 HEPES, 1 EGTA, 0.1 $CaCl_2$, 4 ATP-Na, 0.3 GTP-Na. The pipette holder was attached to the headstage of an Axoclamp 2B amplifier (Molecular Devices, San José, CA, USA) and positioned under visual guidance using a hydraulic micromanipulator (Narishige MHW-13). Signals were low-pass filtered (5 KHz, FL-4 DAGAN Corporation), digitized (40 KHz) using a Digidata 1322A analog-to-digital DAQ device (Molecular Devices, San José, CA, USA) and recorded to a PC using pClamp 8.0 software (Molecular Devices, San José, CA, USA).

To pharmacologically isolate the GABA-mediated inhibitory post-synaptic currents (IPSCs), ionotropic glutamate receptors were blocked by adding kynurenic acid (5 mM, Sigma-Aldrich) to the perfusate. To improve the signal-to-noise ratio of chloride-mediated IPSCs, a 'patch solution' containing 150 mM KCl was used. The Nernst potential for Cl^- (E_{Cl}) and hence, the reversal potential of the GABAergic IPSCs, was estimated as ~ + 5.1 mV at 25°C. Series resistance (typically 10–20 MΩ) was estimated using −10 mV, 20 ms steps from the holding potential (Hamill et al., 1981); recordings were rejected when the series resistance shifted ≥20%. In cell-attached experiments, recording pipettes were filled either with a 150 mM K^+-gluconate based solution -instead of KCl-, or with standard ACSF. Voltage-clamp mode was used in all cell-attached recordings; electrode command potential was 0 mV. Spontaneously firing neurons were recorded while perfusing the slice with regular ACSF (N=3) or with 9 mM KCl-ACSF (see Bracci et al. 1998), giving rise to a steady depolarization-evoked firing (2.24 ± 0.05 Hz, N=3, see **Fig. 1B**). Monopolar stimulating electrodes were pulled from borosilicate glass (tip diameter ≈5 µm), filled with 0.9% saline (NaCl), and positioned in the topographically defined LDT/PPT area—immediately below and near the medial pole of the superior cerebellar peduncle toward the midline and approximately 1 mm dorsal to the PnO core. Monopolar cathodic current pulses were delivered using a constant current unit (ISO-Flex, A.M.P.I.) connected to an Ag/AgCl wire inserted into the saline-filled glass micropipette. Postsynaptic responses were evoked using single pulses, paired-pulse stimulation (ISI=150 ms), or a short train of five pulses at ~15 Hz, with stimuli delivered every 10 s. Stimulation parameters were controlled

with pClamp 8.0 software (typical current pulses ranged from 10–500 pA with durations of 300–400 μs).

Juxtacellular application of drugs.

While recording PnO neurons, single doses of the following drugs were juxtacellularly injected by pressure application (typically 50-150 ms, 5-20 psi), through a glass ejection pipette connected to a Picospritzer III (Parker Instrumentation) and placed between 50 and 100 μm from the recording pipette: (±)-muscarine chloride hydrate (10 μM), (-)-nicotine hydrogen tartrate salt (20 μM), carbamoylcholine chloride (Carbachol, 10 μM), γ-aminobutyric-acid (GABA, 1 mM), 5-(aminomethyl)-1,2-oxazol-3-one (Muscimol, 100 μM), (±)-β-(Aminomethyl)-4-chlorobenzenepropanoic acid (Baclofen, 500 μM). Drugs were purchased from Sigma-Aldrich. Stock solutions were prepared in distilled water, stored at -8°C and diluted in 0,9% NaCl to their final concentration the day of the experiment.

Analysis of IPSCs

Data were analyzed using Clampfit 10.7 (Molecular Devices) and Sigma Plot 11.0 (Systat Software Inc.). To analyze exclusively monosynaptic responses, our study included only IPSCs recorded in the presence of kynurenic acid (5 mM) that met, in addition, the following criteria (adapted from Rose and Metherate, 2005): i) low IPSC onset latency variability (typically SD < 2 ms); ii) no change in IPSC latency with increased stimulus intensity and iii) stable IPSC latency during repetitive (15 Hz) presynaptic stimulation. For a given recorded neuron, the mean peak amplitude of the first (R_1) and subsequent evoked IPSCs (R_2…R_5) elicited by either single or multiple-stimuli protocols (i.e. paired-pulse or short trains), was calculated from 20 consecutive trials (at 0.1 Hz), by averaging the peak values of the corresponding IPSCs. Noise level was taken as ± 5 pA; lower amplitude peak events were considered failures. Given that synaptic failures were included in averaging, the mean peak amplitude of R_i ($i = 1…5$) strictly corresponds to the 'synaptic efficacy' of the *i-th* synaptic event. The latency, coefficient of variation (CV) and the time-constant (τ_{off}) of the decay phase of R_1 were routinely estimated; τ_{off} was estimated by fitting a single exponential function ($y = a*e^{-t/\tau_{off}}$) to the (90–10%) decay phase of the averaged IPSC. The activity-dependent short-term synaptic plasticity

profile (short-term plasticity, STP) was evaluated by calculating the paired-pulse-ratio (PPR = R_2/R_1) from averages of 20 sweeps and the STP-ratio (STPR) in average responses to 20 successive applied trains; the STPR was calculated as a fraction of the mean value of R_3, R_4 and R_5 relative to R_1, i.e., STPR= [1/3 (R_3+ R_4+ R_5)] / R_1. The charge transfer (Q_{inh}, pA.ms), a parameter of synaptic efficacy which incorporates the peak amplitude as well as the time course of synaptic events (Gardner, 1980; Hessler et al., 1993; Rinzel and Rall, 1974), was calculated as the time integral of the membrane current trace for each trial, excluding the stimulus artifact; the mean Q_{inh} was obtained from averages of 20 consecutive trials. Analysis of the effects of cholinergic agonists on IPSCs included: (i) the estimation of changes in synaptic efficacy by comparing evoked changes in functional synaptic parameters measured before (control) and after drug application during its maximal effect, (ii) the evaluation of the pre- or postsynaptic origin of changes in synaptic strength by quantifying changes in the PPR and the STPR, parameters representative of presynaptic function (Bekkers and Stevens, 1990; Davies et al., 1990; Débanne et al., 1996; Dobrunz and Stevens, 1997; Hess et al., 1987; Manabe et al., 1993; Metherate and Ashe, 1994; Schulz et al., 1994; Zucker, 1989, 1973) and changes in $1/CV^2(R_1)$ (Débanne et al., 1996; Faber and Korn, 1991; Malinow and Tsien, 1990). Spontaneous IPSCs (sIPSCs) were analyzed using Clampfit routines. The detection threshold of events was set at 5 pA. The cumulative probability distributions of amplitudes were constructed using 60–120 s gap-free recordings obtained before, immediately following and after (15 min) juxtacellular BACLOFEN application.

Statistical Analysis

Statistical analyses were performed using SigmaPlot 11.0. The significance level was set at $p < 0.05$. Unless otherwise stated, data are presented as mean ± SE and shown in the figures as individual values (i.e., the average for each recorded neuron), where N represents the number of recorded neurons in each experimental series. Changes in synaptic efficacy were evaluated using either the paired Student's t-test or the Wilcoxon signed-rank test, as appropriate, while unpaired data were analyzed using the unpaired Student's t-test or the Mann-Whitney rank sum test.

RESULTS

IPSCs evoked by focal stimulation of the LDT/PPT area

Evoked IPSCs (eIPSCs) were elicited by repetitive stimulation and monitored via whole-cell, voltage-clamp recordings from PnO neurons held at -70 mV. The first eIPSCs (R_1) from either stimulation pattern had a mean latency of 8.54 ± 0.28 ms, a mean amplitude ($R_{1(avg)}$) of 76.75 ± 82.62 pA and a decay time constant of 24.81 ± 1.52 ms (N=51). eIPSCs exhibited a reversal potential of 8.49 ± 5.23 mV (N=3; **Fig.1A**), which closely matched the Nernst potential for Cl^- according to the composition of micropipette internal solution (see Methods). In addition, they were completely blocked by 100 µM picrotoxin (N=3, data not shown), further indicating mediation via $GABA_A$-receptors. Under conditions preserving the physiological chloride concentration gradient (cell-attached recordings), juxta-cellular injections of 1 mM GABA transiently suppressed spontaneous or depolarization-induced action potential firing for approximately 2 seconds (**Fig. 1B**), indicating that GABA-mediated postsynaptic effects were inhibitory. In all experiments, eIPSCs were recorded after blockade of ionotropic glutamatergic transmission (5 mM kynurenic acid), a condition consistent with their monosynaptic nature.

Short term plasticity profile of activated GABAergic synapses

Short-term use-dependent plasticity is a fundamental characteristic of synaptic connections, critically influencing neural network functionality. The dynamics of activated GABAergic synapses were assessed using two distinct stimulation protocols: paired pulses and brief short trains (5 pulses at 15 Hz; see Methods). In most neurons (40/51, ~78%), facilitatory processes predominated (paired-pulse facilitation), with a paired-pulse ratio (PPR) ranging from 1.04 to 2.13, and a mean of 1.37 (± 0.24). Paired-pulse depression was observed in the remaining 11 neurons, with a PPR of 0.88 (± 0.10; range: 0.69–0.98). Overall, the mean PPR across all recorded neurons was 1.27 ± 0.30 (N = 51, **Fig. 1C**). Consistent with established models of use-dependent synaptic plasticity, paired-pulse facilitation -the predominant form of paired-pulse plasticity observed in our experiments- primarily reflects a low initial probability of neurotransmitter release (P_o) (Débanne et al., 1996; Dittman and Regehr, 1998; Silver et al., 1998; Regehr, 2012). In line with this, the PPR exhibited an inverse correlation with $1/CV^2(R1)$, an experimental proxy for P_o (McLachlan, 1978; Faber and Korn, 1991; **Fig. 1D**; *Pearson product moment* correlation: N = 51, r = -0.551, p = 0.0000279). Additionally, also

consistent with a low P_o, R_1 displayed a failure probability of 0.21 ± 0.03, together with substantial amplitude variability (CV(R_1) = 48.08 ± 21.5%; see raw data in **Figs. 1C** and **2A**). Activation of $GABA_B$ autoreceptors by GABA released in response to a presynaptic action potential acts as negative feedback on subsequent GABA release modulating the presynaptic terminal dynamics, thereby influencing paired-pulse plasticity (Davies and Collingridge, 1993; Kobayashi et al., 2012). This possibility was ruled out demonstrating that juxtacellularly-applied microvolumes of 100 μM baclofen, a $GABA_B$-receptor agonist on eIPSCs, had no effect on $R1_{(avg)}$ or the PPR (**Fig. S1A**; *paired t-test: N=9; $R1_{(avg)}$: p=0.89; PPR: p=0.56*). However, baclofen was able to reduce the frequency of spontaneous IPSCs, indicating that GABAB receptors may regulate additional inhibitory GABAergic inputs onto the same postsynaptic cells.

The spiking activity of GABAergic neurons in pontine-mesencephalic areas -including the vlPAG and the LDT/SLD nuclei- varies across the wake-sleep cycle in a state-dependent manner (Boucetta et al., 2014; Weber et al., 2018). In naturally sleeping-waking rats glutamic acid decarboxylase-positive ($GAD^{+)}$ neurons in the SLD exhibit REM sleep-specific (REM-S) and wake/REM sleep-specific (W/REM-S) maximal activity, firing in short bursts of action potential at ~15–20 Hz (Boucetta et al., 2014). Therefore, short-term, use-dependent plasticity of activated GABAergic synapses was also examined using short trains stimulation protocols (**Fig. 2A**), as an experimental proxy for 'nearly physiological regimes' of presynaptic activation (N=57). On average, eIPSCs exhibited frequency facilitation, with a short-term plasticity ratio (STPR) of 1.32 ± 0.72 (**Fig. 2A**, right). This average behavior -also illustrated in **Fig. 2D-** comprises a subset of neurons (36/57) displaying facilitation across the stimulation train (see the representative example **in Fig. 2A**, left) with a STPR of 1.69 ± 0.65 (range: 1.01 - 3.34). The remaining neurons (21/57) exhibited frequency depression with a STPR of 0.68 ± 0.17 (range: 0.31-0.98). As for the PPR, the STPR correlated negatively with $1/CV^2(R_1)$ (*Pearson product moment correlation: N=57, r=-0.525, p=0.0000763,* **Fig. 2B***).* Neither $R_{1(avg)}$ (68.92 ± 52.99 pA, **Fig.2A**, right) nor PPR (1.23 ± 0.46, not shown) from this dataset differed significantly from paired-pulse stimulation datasets (*Mann-Whitney rank sum test: R_1: p=0.744; PPR: p=0.225*). Therefore, data from paired-pulse and short train stimulation experiments (N=108) were pooled for further analysis of the presynaptic dynamics of activated GABAergic inputs. As expected, PPR and $1/CV^2(R_1)$ showed significant correlation (*Pearson product moment correlation: r=-0.257, p=0.00729*). In contrast, the PPR and $R_{1(avg)}$ were not correlated (*Pearson product moment correlation: r=-0.176, p=0.0681* suggesting that short-term plasticity profiles are independent of R1

amplitude and thus unaffected by eventual variations of focal stimulation (Kim and Alger, 2001). This notion finds further support in the fact that neurons exhibiting paired-pulse facilitation (PPR>1) and paired-pulse depression (PPR<1) differed significantly in $1/CV^2(R_1)$ but not in $R_{1(avg)}$ (**Fig.2C;** *Mann-Whitney rank sum test: PPD: N=29; PPF: N=79;* $1/CV^2(R_1)$*: p=0.001;* $R_{1(avg)}$*: p= 0.084*). **Figure 2D** summarizes the short-term plasticity profiles of GABAergic synapses activated during the application of short trains stimulation protocols, highlighting the predominant short-term facilitation (i.e. PPR>1 and STPR>1, shaded area).

Collectively, these findings suggest that most GABAergic inputs activated by focal stimulation of the LDT/PPT area are mediated by a specialized subset of synapses characterized by a low release probability (as indicated by low $1/CV^2$ values for R_1) and use-dependent facilitation (with PPR > 1 and STPR > 1) as the predominant short-term plasticity profile.

Cholinergic modulation of GABAergic transmission at the PnO.

The effects of juxta-cellular microvolume injections of the cholinergic agonists carbachol (CCh, 1 mM), muscarine (10 µM), and nicotine (20 µM) on $R_{1(avg)}$ and on short-term presynaptic plasticity indices -namely, the paired-pulse ratio (PPR) and short-term plasticity ratio (STPR)- were evaluated using both paired-pulse and short train stimulation protocols.

Microinjections of CCh, a non-selective muscarinic and nicotinic acetylcholine (ACh) receptor agonist, were performed in N=28 experiments. The cholinergic challenge induced transient modifications in $R_{1(avg)}$ in all experiments (28 out of 28) that consisted either in reductions or enhancements. Importantly, these changes in synaptic efficacy were consistently accompanied by changes in the PPR -either increases or decreases- strongly suggesting a presynaptic mechanism of action. In addition, in experiments where CCh effects were evaluated on IPSCs evoked by juxta-cellular injections of GABA (data not shown), nor $R_{1(avg)}$ (87.16 ± 9.09 % of control, *paired t-test: N=10, p=0.19*) nor the eIPSCs decay time constant (115.84 ± 7.60 % of control, *N=10, p=0.14*) showed significant changes, indicating a negligible involvement of post-synaptic effects. When data were pooled, CCh produced no net effect on $R_{1(avg)}$ (69.17 ± 63.50 pA before, 61.93 ± 74.42 pA after injection; *paired t-test: p=0.09*), nor on the PPR (1.39 ± 0.40 before, 1.33 ± 0.45 after injection; *Wilcoxon signed-rank test: p=0.078*). However, a significant decrease in $R_{1(avg)}$ was observed in 20 out of 28 neurons at 9.08 ± 0.62 minutes post-injection (−31.35 ± 20.25%; *Wilcoxon signed-rank test: p < 0.001*; **Fig. 3A1**). In these neurons, the reduction in $R_{1(avg)}$ was associated with either an increase

in the PPR (+27.68 ± 12.36%; p = 0.002, N = 7) or a decrease in the PPR (−34.50 ± 5.37%; *p < 0.001, N = 13*; **Fig. 3A2**). In the remaining experiments (N = 8), $R_{1(avg)}$ increased (+4.77 ± 9.65%; *p = 0.008;* **Fig. 3B1**), with these changes accompanied by variable, albeit non-significant, modifications in the PPR (an increase of +221.91 ± 186.75%, *p = 0.315, N = 3;* or a decrease of −19.61 ± 7.46%, *p = 0.085, N = 5*; **Fig. 3B2**). Effects of CCh dissipated almost completely by 19.23 ± 0.89 minutes after injection.

Activation of presynaptic muscarinic (mAChRs) and nicotinic (nAChRs) acetylcholine receptors can differentially modulate the initial release probability (P_0) of synaptic terminals, thereby influencing their short-term synaptic plasticity profiles. We hypothesized that the diverse effects of CCh on GABAergic transmission are mediated by the differential activation of presynaptic mAChRs and nAChRs. Accordingly, we evaluated the effects of selectively activating these receptors on evoked inhibitory postsynaptic currents (eIPSCs). Juxta-cellular application of muscarine (10 μM) reversibly decreased $R_{1(avg)}$ in all experiments (-36.28 ± 18.88 %; *Wilcoxon signed-rank test: p < 0.001, N=15;* **Fig. 4A1**), whereas nicotine (20 μM) produced an opposite effect increasing $R_{1(avg)}$ by +39.12 ± 24.65% (*p<0.001, N=14;* **Fig. 4B1)**. The maximal changes in $R_{1(avg)}$ were observed at 7.54 ± 3.90 for muscarine and 2.75 ± 2.07 minutes for nicotine. Muscarine-induced decreases in $R_{1(avg)}$ were consistently accompanied by increases in the PPR (+21.80 ± 5.1 %, *p=0.004; N=8*; **Fig. 4A2**, left), whereas nicotine systematically reduced the PPR (-10.94 ± 1.79%; *p=0.003; N=8;* **Fig. 4B2,** left). Additionally, muscarine and nicotine induced opposite changes in the short-term plasticity ratio (STPR) of IPSCs evoked at 15 Hz, consistent with their opposing effects on P_0 (**Figs. 4A2** and **B2**, middle panels**;** muscarine: +93.32 ± 62.53 %, *paired t-test: p = 0.031, N=7;* nicotine: -31.48 ± 2.17 %, *p = 0.031, N=6*). These effects did not appear to correlate with the initial PPR or STPR values (see initial values in **Figs. 4A2** and **B2**).

The above results demonstrate the cholinergic modulation of activated GABAergic inputs to PnO neurons via presynaptic mAChRs and nAChRs. Activation of these cholinergic receptors elicited opposite-direction changes in $R1_{(avg)}$ as well as in the PPR/STPR, thereby changing presynaptic terminal dynamics. We next aimed to assess whether muscarinic and nicotinic modulation leads to net depression or facilitation of the inhibitory effect on postsynaptic neurons during repetitive activation of GABAergic inputs. To this end, we quantified changes in the total inhibitory charge transfer ($Q_{inh.}$) induced by muscarine (N = 6) and nicotine (N = 6) during short-train stimulation. The total charge transfer, which represents the cumulative movement of charge across the membrane

during postsynaptic currents, serves as a proxy for the amount of neurotransmitter released, thereby providing an estimate of the net functional impact of synaptic inputs on postsynaptic outputs.

Despite the opposing effects observed on $R_{1(avg)}$, PPR, and STPR, both muscarine and nicotine consistently decreased Q_{inh}, although the reduction observed with muscarine did not reach statistical significance (muscarine: -15.15 ± 18.71 %, *paired t-test: p=0.145, N=6*; nicotine: -13.74 ± 3.91 %; *p=0.038, N=6;* **Figs. 4A2** and **B2**, right panels).

DISCUSSION

Many previous studies highlight the interaction between W-promoting GABAergic and REM-S-promoting cholinergic processes at REM-S executive brainstem areas (Xi et al., 2004; Vazquez and Baghdoyan, 2004; Fuller et al., 2007; Fenik and Kubin, 2009; Vanini et al., 2011; 2013; Weber et al., 2018). Considerable evidence has accumulated supporting a gating REM-S role of GABAergic innervation of REM-on PnO reticular neurons, whose activity results in the regulation of the onset and offset of REM-S and probably also in the maintenance of this behavioral state (Sastre et al., 1996; Boissard et al., 2003; Pollock and Mistlberger, 2003; Sanford et al., 2003; Xi et al., 2004; Sapin et al., 2009; see for a review Luppi et al., 2011). In contrast to the wealth of data showing that cholinergic transmission at the PnO is under GABAergic control (Vazquez and Baghdoyan, 2004; Marks et al., 2008; Flint et al., 2010; Liang and Marks, 2014), the cholinergic modulation of GABAergic inputs to PnO neurons has not been yet specifically addressed. This cholinergic control of GABAergic transmission may be considered as part of a mutual inhibitory interaction between GABAergic and cholinergic processes in REM-S executive brainstem areas, as suggested by behavioral studies.

Our main findings include the following: (1) focal stimulation in a restricted mesopontine area near the medial pole of the superior cerebellar peduncle evoked monosynaptic IPSCs at PnO neurons, likely mediated by $GABA_A$ receptors and with inhibitory postsynaptic effects on PnO neurons; (2) the vast majority of these inputs (~70%) result from activation of GABAergic terminals with low probability of transmitter release, short-term activity-dependent facilitation and lacking presynaptic modulation mediated by GABAB receptors; (3) activated GABAergic inputs targeting PnO neurons are apparently endowed with functional, presynaptic mAChRs and nAChRs whose activation modulates the probability of GABA release in opposite directions: is decreased via activation of mAChRs and increased through the activation of nAChRs; (4) under physiological regimes of presynaptic activity, however, activation of both receptor subtypes lead to a reduction of inhibition of PnO neurons.

Characteristics of activated GABAergic inputs in putative REM-on PnO neurons.

Previous electrophysiological studies addressed the analysis, of membrane potential changes of PnO neurons evoked by the local application of GABA (Nuñez et al., 1988), the occurrence of

spontaneous postsynaptic responses at these cells (Brown et al., 2006) and the modulation by carbachol of spontaneous IPSCs and IPSCs evoked by stimuli applied close to the recorded cells (Heister et al., 2009). Weng et al. (2014) analyzed the cholinergic modulation of spontaneous postsynaptic currents but, specifically, in spinally projecting pontine reticular neurons. In our study, we performed an in-depth analysis of functional properties and the cholinergic modulation of a subset of GABAergic inputs to putative REM-on PnO evoked by focal electrical stimulation in a restricted area near the medial pole of the superior cerebellar peduncle. In addition to meeting the electrophysiological inclusion criteria adapted from Rose y Metherate (2005), evoked IPSCs (eIPSCs) were recorded under 5 mM kynurenic acid, a condition supporting their monosynaptic nature. Our data indicates that eIPSCs cause postsynaptic inhibition at PnO neurons, implying $GABA_A$ receptors (**Fig. 1**). The prevalent expression of facilitation during paired-pulse and short train stimulation (**Figs. 1** and **2**), together with a relatively high CV(R_1) and a considerable probability of failure of synaptic transmission, indicates that eIPSCs result from the activation of a specialized subset of low-P_0 GABAergic terminals (Bekkers and Stevens, 1990; Davies et al., 1990; Faber and Korn, 1991; Débanne et al., 1996; Dobrunz and Stevens, 1997).

Although the origin of the activated GABAergic projections was not specifically investigated in this study, the stimulation site suggests that both GABAergic neurons from the LDT and the axonal processes of GABAergic neurons of the vlPAG and the LPT were likely activated. Substantial evidence supports the role of these structures in controlling REM sleep executive areas (Semba, 1993; Sastre et al., 1996; Boissard et al., 2003; Lu et al., 2006; Vanini et al 2007; Sapin et al., 2009; Pino et al., 2017; Weber et al., 2018). While most GABAergic neurons in these regions are considered REM-off -meaning their activity is drastically reduced during REM sleep and they are likely responsible for inhibiting REM sleep executive areas- a subset is classified as REM-on (Lu et al., 2006b; Sapin et al., 2009; Boucetta et al., 2014; Weber et al., 2018). REM-on GABAergic neurons in the vlPAG or LPT are thought to inhibit brainstem monoaminergic REM-off (wake-promoting) structures (such as the dorsal raphe and locus coeruleus) and, possibly, GABAergic interneurons in the PnO that are likely involved in the tonic inhibition of REM sleep effector neurons (Weber et al., 2015, 2018).

Among other physiological functions, short-term synaptic plasticity has been implicated in synaptic computation by filtering the transmission of information between neurons (Fortune and Rose, 2001). This is particularly relevant during repetitive presynaptic activity. Synapses with a low initial

probability of neurotransmitter release, exhibit frequency facilitation and function as high-pass filters, whereas synapses with a high initial probability of release, show frequency depression, acting as low-pass filters (Fortune and Rose, 2001; Abbott and Regehr, 2004; Monday et al., 2018). Here, the short-term plasticity profile of most GABAergic synaptic inputs to PnO neurons (**Fig. 2D**) suggests that they may function as high-pass filters that favor GABAergic inhibition of neuronal targets during periods of repetitive presynaptic activity. Interestingly, evidence obtained *in vivo* indicates that the spiking activity of brainstem GABAergic cell groups thought to innervate REM-S executive areas are strongly modulated by the sleep-wake cycle (Boucetta et al., 2014; Weber et al., 2018). Characteristically, REM-sleep related cells exhibit short periods of repetitive discharge of action potentials at 15-20 s^{-1} (Boucetta et al., 2014; Luppi et al., 2017; Jones, 2017; Weber et al. 2018; Blanco-Centurion et al; 2023).

Presynaptic mAChRs and nAChRs mediate cholinergic modulation of activated GABAergic inputs.

In the present study, we found that CCh consistently elicited transient changes in the efficacy of GABAergic synapses. Although this phenomenon was observed in all tested PnO neurons, the changes in $R1_{(avg)}$ amplitude were not homogeneous: CCh reduced $R1_{(avg)}$ amplitude (depression) in 20 out of 28 neurons (71%, **Fig. 3A)** while enhancing $R1_{(avg)}$ (facilitation) in the remaining 8 cells (29%,**Fig. 3C**). In all cases, changes in $R1_{(avg)}$ were accompanied by changes in the PPR, indicative of a presynaptic mechanism (**Fig. 3B and D**). This conclusion is further supported by the absence of changes in membrane currents evoked by the juxtacellular application of GABA microvolumes in the presence of CCh. Our findings complement those of Sandford et al. (2003) and provide further experimental support for a functional interaction between cholinergic and GABAergic innervation of the PnO, as reported in several studies (e.g., Xi et al., 2004; Marks et al., 2008; Vanini et al., 2011; reviewed in Watson et al., 2011 and Brown et al., 2012).

Due to its non-selectivity, CCh likely exerts a range of effects on GABAergic synaptic transmission, including those mediated by the activation of presynaptic muscarinic (mAChRs) and nicotinic (nAChRs) receptors -with muscarine replicating synaptic depression and nicotine facilitating transmission (Fig. 4). However, the effects of CCh on the short-term plasticity profile associated with modulations in $R_{1(avg)}$ challenge this interpretation. In fact, synaptic depression accompanied by an

increased paired-pulse ratio (PPR) -indicative of a presynaptic muscarinic effect- was observed in only 7 neurons, whereas a nicotinic presynaptic effect -facilitation with a decrease of the PPR- was detected in 5 neurons. In summary, a net prevailing muscarinic or nicotinic presynaptic effect of CCh might account for results observed in 12 out of 28 neurons (43% with opposite shifts in $R_{1(avg)}$ and the PPR) whereas in the remaining 57% of neurons, CCh effects on $R_{1(avg)}$ and the PPR are compatible with a diverse combination of muscarinic or nicotinic presynaptic effects (Chen et al., 2002; Rozov and Burnashev, 1999).

mAChRs are G protein-coupled receptors that can be subdivided into two groups (Assous, 2021). The M1-like receptors group (including M1, M3, and M5 receptors) are coupled to Gq/11 G-proteins, and usually associated with excitatory neural effects mediated by activation of protein kinase C and phospholipase C. The M2-like receptors group (including M2 and M4 type receptors) are coupled to Gi/o G proteins inhibiting adenylyl cyclase and are implicated in inhibitory effects. At synaptic level, activation of the M2-like group mediated presynaptic inhibition through inhibition of voltage-dependent Ca^{2+} channels leading to a reduction of evoked neurotransmitter release probability. Neuronal nAChRs are ionotropic receptors permeable to Na^{+}, K^{+}, and Ca^{2+} ions that mediate fast synaptic transmission and, most importantly, intracellular signaling via Ca^{2+}-dependent signaling pathways (Wonnacott, 1997; Dajas-Bailador and Wonnacott, 2004; Gotti et al., 2009; Zoli et al., 2018). Activation of nAChRs at presynaptic level causes a rise in the cytosolic Ca^{2+} leading to an increase in release probability via the modulation of several critical steps in neurotransmitter release. At the brainstem mesopontine region, a large body of evidence indicates the existence of cholinoceptive structures whose pharmacological manipulation causes changes in the occurrence and timing of REM-S episodes (reviewed in Brown et al., 2012; Luppi et al., 2012; Weber et al., 2018; Wang et al., 2021). Experimental data obtained using different approaches including *in vivo* and *in vitro* models, indicate that cholinergic modulation of sleep related mesopontine structures may involve both mAChRs (M1 and M2-like groups) and nAChRs (probably α4β2) (Greene et al., 1985; Stevens et al., 1993; Gillin et al., 1993; McCarley et al., 1995; Brischoux et al., 2008; Léna et al., 2004; Coleman et al., 2004; Heister et al., 2009; Brown et al., 2012).

Our data indicate that GABAergic terminals contacting PnO neurons are modulated by two distinct cholinergic receptor systems. Activation of M2-like muscarinic acetylcholine receptors (mAChRs) produces presynaptic inhibition, as evidenced by a reduction in $R1_{(avg)}$ and corresponding increases in both PPR and STPR (Fig. 4A and B). In contrast, activation of nicotinic acetylcholine receptors

(nAChRs) mediates presynaptic facilitation, as indicated by an increase in R1(avg) coupled with reduced PPR and STPR (Fig. 4C and D). Given that mAChRs and nAChRs utilize independent intracellular signaling mechanisms, co-activation of both receptor types by CCh -when they are co-expressed at the same presynaptic terminals- may result in a combination of their respective cellular effects. Moreover, dual muscarinic/nicotinic effects of CCh -characterized by shifts in both $R_{1(avg)}$ and the short-term plasticity profile in the same direction (**Fig. 3**)- observed in 57% of neurons, may depend on the simultaneous activation of mAChRs and nAChRs at these terminals. Modulation of synaptic transmission mediated by activation of different presynaptic receptor subtypes with opposing effects on transmitter release has been described in other neural structures (Zhang and Warren, 2002; Bono et al, 2023). The predominance of the effects mediated by one receptor over the other on $R_{1(avg)}$ and the short-term plasticity profile depends, among other factors, on each receptor type's expression level and the functional state of the terminals (including intracellular signaling pathways; Perrins and Roberts, 1994; Grilli et al., 2009; Marchi and Grilli, 2010).

It is worth noting that despite the opposing effects of presynaptic activation of mAChRs (depression) and nAChRs (facilitation) on GABAergic transmission at the PnO, activation of either cholinergic receptor subtype during presynaptic activation mimicking physiological activity patterns of REM-off GABAergic neurons (Boucetta et al., 2014; Weber et al., 2018), reduced the inhibitory drive onto PnO neurons (as represented by Q_{inh} in **Fig. 4**). Thus, it is reasonable to speculate that an increased cholinergic tone during the transition from non-REM to REM-S leads to a local inhibition of GABA release via the co-activation of presynaptic mAChRs and nAChRs. This scenario is plausible because volume transmission likely constitutes the dominant mode of transmission at the target regions of cholinergic projections in brainstem neural circuits involved in REM sleep control (Saper and Fuller, 2017), as well as in other CNS regions (Picciotto et al, 2012; Bennett et al., 2012; Lendvai and Vizi, 2008; Yamasaki et al., 2010; Liang and Marks, 2014). Although our data strongly suggest that mAChRs and nAChRs are co-expressed in the same GABAergic presynaptic terminals, a definitive demonstration requires further analysis of cholinergic modulation of GABA transmission using complementary approaches, such as the minimal stimulation method, which activates a single or only a few presynaptic axons (Raastad et al., 1992).

Possible functional implications of our data

The mutual inhibition model (or flip-flop switch model; Lu et al., 2006) has provided seminal conceptual frameworks for advancing the study of sleep mechanisms (Fuller et al., 2007; Brown et al., 2012; Weber and Dan, 2016; Héricé et al., 2019; Weber, 2017). This model consists of mutually inhibitory interactions between REM-S-promoting and REM-S-inhibiting neuronal structures. Although recent evidence points to dual GABAergic/glutamatergic control of REM sleep-promoting mesopontine structures, the REM-S sleep-promoting effect of cholinergic innervation of these structures interacting with GABAergic REM-S-suppressive influences still has considerable support (Mark and Sinton, 2010; Vanini et al., 2011; Arrigoni et al., 2016; Peever and Fuller, 2017; Weber et al., 2018; Arrigoni and Fuller, 2019; Grace and Horner, 2020). While the application of cholinergic agonists in this area is associated with a REM-S facilitating effect (not triggering), GABA agonists have a clear REM-S-suppressive effect (see *Introduction*). A local mutual inhibition between GABAergic and cholinergic inputs to the PnO is consistent with their antagonistic effect on REM-S. Inhibition of ACh release from cholinergic terminals by GABA has been proposed based on electrophysiological, pharmacological, and immunolabeling evidence (Vazquez and Baghdoyan, 2004; Marks et al., 2008; Flint et al., 2010; Vanini et al., 2011; Liang and Marks, 2014). In this study, we demonstrate that GABAergic terminals in contact with PnO neurons are under intricate cholinergic presynaptic regulation, in line with a design of local, presynaptic mutual inhibition between GABAergic and cholinergic inputs to the PnO.

The transition from non-REM to REM-S is characterized by a progressive increase in the activity of REM-on neurons in the mesopontine reticular region under cholinergic influence, along with a progressive reduction in the firing rate of REM-off GABAergic neurons of the vlPAG and the LPT, mediating the gating of REM sleep (Weber et al., 2018). The net presynaptic inhibition of GABAergic inputs mediated by the activation of cholinergic receptors may have a role in controlling the characteristics and duration of this transition (Fraigne and Peever, 2015). Moreover, together with the presynaptic GABAergic inhibition of cholinergic terminals at the PnO, the cholinergic relief of GABAergic inhibition could offer a mechanism of local mutual inhibition at the presynaptic level between GABAergic and cholinergic terminals at the PnO, with possible relevant functional consequences on the ultradian rhythm of non-REM/REM alternation (Brown et al., 2012; Luppi et al., 2012; Weber et al., 2018; Wang et al., 2021).

REFERENCES

Abbott, L. F., & Regehr, W. G. (2004). Synaptic computation. Nature, 431(7010), 796-803. https://doi.org/10.1038/nature03010

Arrigoni, E., & Fuller, P. M. (2019). The Circuit, Cellular, and Synaptic Bases of Sleep-Wake Regulation. In Handbook of Behavioral Neuroscience (Vol. 30, pp. 65-88). Elsevier. https://doi.org/10.1016/B978-0-12-813743-7.00005-0

Arrigoni, E., Chen, M. C., & Fuller, P. M. (2016). The anatomical, cellular and synaptic basis of motor atonia during rapid eye movement sleep. The Journal of physiology, 594(19), 5391-5414. https://doi.org/10.1113/JP271324

Assous, M. (2021). Striatal cholinergic transmission. Focus on nicotinic receptors' influence in striatal circuits. European Journal of Neuroscience, 53(8), 2421-2442. https://doi.org/10.1111/ejn.15135

Bekkers, J. M., & Stevens, C. F. (1990). Presynaptic mechanism for long-term potentiation in the hippocampus. Nature, 346(6286), 724-729. https://doi.org/10.1038/346724a0

Bennett, C., Arroyo, S., Berns, D., & Hestrin, S. (2012). Mechanisms generating dual-component nicotinic EPSCs in cortical interneurons. Journal of Neuroscience, 32(48), 17287-17296. https://doi.org/10.1523/JNEUROSCI.3565-12.2012

Blanco-Centurion, C., Vidal-Ortiz, A., Sato, T., & Shiromani, P. J. (2023). Activity of GABA neurons in the zona incerta and ventral lateral periaqueductal grey is biased towards sleep. Sleep, 46(3), zsac306. https://doi.org/10.1093/sleep/zsac306

Boissard, R., Gervasoni, D., Schmidt, M. H., Barbagli, B., Fort, P., & Luppi, P. H. (2002). The rat ponto-medullary network responsible for paradoxical sleep onset and maintenance: a combined microinjection and functional neuroanatomical study. European Journal of Neuroscience, 16(10), 1959-1973. https://doi.org/10.1046/j.1460-9568.2002.02257.x

Boissard, R., Fort, P., Gervasoni, D., Barbagli, B., & Luppi, P. H. (2003). Localization of the GABAergic and non-GABAergic neurons projecting to the sublaterodorsal nucleus and potentially gating paradoxical sleep onset. European Journal of Neuroscience, 18(6), 1627-1639. https://doi.org/10.1046/j.1460-9568.2003.02861.x

Bono, F., Fiorentini, C., Mutti, V., Tomasoni, Z., Sbrini, G., Trebesova, H., ... & Missale, C. (2023). Central nervous system interaction and crosstalk between nAChRs and other ionotropic and metabotropic neurotransmitter receptors. Pharmacological Research, 190, 106711. https://doi.org/10.1016/j.phrs.2023.106711

Boucetta, S., Cissé, Y., Mainville, L., Morales, M., & Jones, B. E. (2014). Discharge profiles across the sleep-waking cycle of identified cholinergic, GABAergic, and glutamatergic neurons in the pontomesencephalic tegmentum of the rat. Journal of Neuroscience, 34(13), 4708-4727. https://doi.org/10.1523/JNEUROSCI.2617-13.2014

Brischoux, F., Mainville, L., & Jones, B. E. (2008). Muscarinic-2 and orexin-2 receptors on GABAergic and other neurons in the rat mesopontine tegmentum and their potential role in sleep-wake state control. Journal of Comparative Neurology, 510(6), 607-630. https://doi.org/10.1002/cne.21803

Brown, R. E., McKenna, J. T., Winston, S., Basheer, R., Yanagawa, Y., Thakkar, M. M., & McCarley, R. W. (2008). Characterization of GABAergic neurons in rapid-eye-movement sleep controlling regions of the brainstem reticular formation in GAD67-green fluorescent protein knock-in mice. European Journal of Neuroscience, 27(2), 352-363. https://doi.org/10.1111/j.1460-9568.2008.06024.x

Brown, R. E., Basheer, R., McKenna, J. T., Strecker, R. E., & McCarley, R. W. (2012). Control of sleep and wakefulness. Physiological reviews. https://doi.org/10.1152/physrev.00032.2011

Chen, C. Y., Ling, E. H., Horowitz, J. M., & Bonham, A. C. (2002). Synaptic transmission in nucleus tractus solitarius is depressed by Group II and III but not Group I presynaptic metabotropic glutamate receptors in rats. The Journal of physiology, 538(3), 773-786. https://doi.org/10.1113/jphysiol.2001.012948

Coleman, C. G., Lydic, R., & Baghdoyan, H. A. (2004). M2 muscarinic receptors in pontine reticular formation of C57BL/6J mouse contribute to rapid eye movement sleep generation. Neuroscience, 126(4), 821-830. https://doi.org/10.1016/j.neuroscience.2004.04.029

Dajas-Bailador, F., & Wonnacott, S. (2004). Nicotinic acetylcholine receptors and the regulation of neuronal signalling. Trends in pharmacological sciences, 25(6), 317-324. https://doi.org/10.1016/j.tips.2004.04.006

Davies, C. H., Davies, S. N., & Collingridge, G. L. (1990). Paired-pulse depression of monosynaptic GABA-mediated inhibitory postsynaptic responses in rat hippocampus. The Journal of physiology, 424(1), 513-531. https://doi.org/10.1113/jphysiol.1990.sp018080

Débanne, D., Guérineau, N. C., Gähwiler, B. H., & Thompson, S. M. (1996). Paired-pulse facilitation and depression at unitary synapses in rat hippocampus: quantal fluctuation affects subsequent release. The Journal of physiology, 491(1), 163-176. https://doi.org/10.1113/jphysiol.1996.sp021204

Dittman, J. S., & Regehr, W. G. (1998). Calcium dependence and recovery kinetics of presynaptic depression at the climbing fiber to Purkinje cell synapse. Journal of Neuroscience, 18(16), 6147-6162. https://doi.org/10.1523/JNEUROSCI.18-16-06147.1998

Dobrunz, L. E., & Stevens, C. F. (1997). Heterogeneity of release probability, facilitation, and depletion at central synapses. Neuron, 18(6), 995-1008. https://doi.org/10.1016/S0896-6273(00)80338-4

Korn, H., & Faber, D. S. (1991). Quantal analysis and synaptic efficacy in the CNS. Trends in neurosciences, 14(10), 439-445. https://doi.org/10.1016/0166-2236(91)90042-S

Fenik, V. B., & Kubin, L. (2009). Differential localization of carbachol-and bicuculline-sensitive pontine sites for eliciting REM sleep-like effects in anesthetized rats. Journal of sleep research, 18(1), 99-112. https://doi.org/10.1111/j.1365-2869.2008.00687.x

Flint, R. R., Chang, T., Lydic, R., & Baghdoyan, H. A. (2010). GABAA receptors in the pontine reticular formation of C57BL/6J mouse modulate neurochemical, electrographic, and behavioral phenotypes of wakefulness. Journal of Neuroscience, 30(37), 12301-12309. https://doi.org/10.1523/JNEUROSCI.1119-10.2010

Fortune, E. S., & Rose, G. J. (2001). Short-term synaptic plasticity as a temporal filter. Trends in neurosciences, 24(7), 381-385. https://doi.org/10.1016/S0166-2236(00)01835-X

Fraigne, J. J., Torontali, Z. A., Snow, M. B., & Peever, J. H. (2015). REM sleep at its core-circuits, neurotransmitters, and pathophysiology. Frontiers in neurology, 6, 123. https://doi.org/10.3389/fneur.2015.00123

Fuller, P. M., Saper, C. B., & Lu, J. (2007). The pontine REM switch: past and present. The Journal of physiology, 584(3), 735-741. https://doi.org/10.1113/jphysiol.2007.140160

Gillin, J. C., Salin-Pascual, R., Velazquez-Moctezuma, J., Shiromani, P., & Zoltoski, R. (1993). Cholinergic receptor subtypes and REM sleep in animals and normal controls. Progress in brain research, 98, 379-387. https://doi.org/10.1016/S0079-6123(08)62422-X

Gotti, C., Clementi, F., Fornari, A., Gaimarri, A., Guiducci, S., Manfredi, I., ... & Zoli, M. (2009). Structural and functional diversity of native brain neuronal nicotinic receptors. Biochemical pharmacology, 78(7), 703-711. https://doi.org/10.1016/j.bcp.2009.05.024

Grace, K. P., & Horner, R. L. (2020). A focal inactivation and computational study of ventrolateral periaqueductal gray and deep mesencephalic reticular nucleus involvement in sleep state switching and bistability. Eneuro, 7(6). https://doi.org/10.1523/ENEURO.0451-19.2020

Greene, R. W., & Carpenter, D. O. (1985). Actions of neurotransmitters on pontine medical reticular formation neurons of the cat. Journal of neurophysiology, 54(3), 520-531. https://doi.org/10.1152/jn.1985.54.3.520

Grilli, M., Pittaluga, A., Merlo-Pich, E., & Marchi, M. (2009). NMDA-mediated modulation of dopamine release is modified in rat prefrontal cortex and nucleus accumbens after chronic nicotine treatment. Journal of neurochemistry, 108(2), 408-416. https://doi.org/10.1111/j.1471-4159.2008.05792.x

Heister, D. S., Hayar, A., & Garcia-Rill, E. (2009). Cholinergic modulation of GABAergic and glutamatergic transmission in the dorsal subcoeruleus: mechanisms for REM sleep control. Sleep, 32(9), 1135-1147. https://doi.org/10.1093/sleep/32.9.1135

Héricé, C., Patel, A. A., & Sakata, S. (2019). Circuit mechanisms and computational models of REM sleep. Neuroscience Research, 140, 77-92. https://doi.org/10.1016/j.neures.2018.08.003

Jones, B. E. (2017). Principal cell types of sleep-wake regulatory circuits. Current opinion in neurobiology, 44, 101-109. https://doi.org/10.1016/j.conb.2017.03.018

Jones, B. E. (2020). Arousal and sleep circuits. Neuropsychopharmacology, 45(1), 6-20. https://doi.org/10.1038/s41386-019-0444-2

Kim, J., & Alger, B. E. (2001). Random response fluctuations lead to spurious paired-pulse facilitation. Journal of Neuroscience, 21(24), 9608-9618. https://doi.org/10.1523/JNEUROSCI.21-24-09608.2001

Léna, C., Popa, D., Grailhe, R., Escourrou, P., Changeux, J. P., & Adrien, J. (2004). β2-Containing nicotinic receptors contribute to the organization of sleep and regulate putative micro-arousals in mice. Journal of Neuroscience, 24(25), 5711-5718. https://doi.org/10.1523/JNEUROSCI.3882-03.2004

Lendvai, B., & Vizi, E. S. (2008). Nonsynaptic chemical transmission through nicotinic acetylcholine receptors. Physiological reviews, 88(2), 333-349. https://doi.org/10.1152/physrev.00040.2006

Liang, C. L., & Marks, G. A. (2009). A novel GABAergic afferent input to the pontine reticular formation: the mesopontine GABAergic column. Brain research, 1297, 32-40. https://doi.org/10.1016/j.brainres.2009.08.045

Liang, C. L., & Marks, G. A. (2014). GABAA receptors are located in cholinergic terminals in the nucleus pontis oralis of the rat: implications for REM sleep control. Brain research, 1543, 58-64. https://doi.org/10.1016/j.brainres.2013.10.019

Lu, J., Sherman, D., Devor, M., & Saper, C. B. (2006). A putative flip-flop switch for control of REM sleep. Nature, 441(7093), 589-594. https://doi.org/10.1038/nature04767

Luppi, P. H., Gervasoni, D., Verret, L., Goutagny, R., Peyron, C., Salvert, D., ... & Fort, P. (2006). Paradoxical (REM) sleep genesis: the switch from an aminergic-cholinergic to a GABAergic-glutamatergic hypothesis. Journal of Physiology-Paris, 100(5-6), 271-283. https://doi.org/10.1016/j.jphysparis.2007.05.006

Luppi, P. H., & Fort, P. (2011). The Neurobiology of Sleep-Wake Systems: An Overview. Narcolepsy: Pathophysiology, Diagnosis, and Treatment, 107-119. https://doi.org/10.1007/978-1-4419-8390-9_10

Luppi, P. H., Clement, O., Sapin, E., Peyron, C., Gervasoni, D., Léger, L., & Fort, P. (2012). Brainstem mechanisms of paradoxical (REM) sleep generation. Pflügers Archiv-European Journal of Physiology, 463, 43-52. https://doi.org/10.1007/s00424-011-1054-y

Luppi, P. H., Peyron, C., & Fort, P. (2017). Not a single but multiple populations of GABAergic neurons control sleep. Sleep medicine reviews, 32, 85-94. https://doi.org/10.1016/j.smrv.2016.03.002

Luppi, P. H., Chancel, A., Malcey, J., Cabrera, S., Fort, P., & Maciel, R. M. (2024). Which structure generates paradoxical (REM) sleep: The brainstem, the hypothalamus, the amygdala or the cortex?. Sleep Medicine Reviews, 74, 101907. https://doi.org/10.1016/j.smrv.2024.101907

Marchi, M., & Grilli, M. (2010). Presynaptic nicotinic receptors modulating neurotransmitter release in the central nervous system: functional interactions with other coexisting receptors. Progress in neurobiology, 92(2), 105-111. https://doi.org/10.1016/j.pneurobio.2010.06.004

Marks, G. A., & Sinton, C. M. (2010). The Role of GABAergic Modulation of Mesopontine Cholinergic Neurotransmission in Rapid Eye Movement (REM) Sleep. GABA and sleep: molecular, functional and clinical aspects, 253-277. https://doi.org/10.1007/978-3-0346-0226-6_12

Marks, G. A., Sachs, O. W., & Birabil, C. G. (2008). Blockade of GABA, type A, receptors in the rat pontine reticular formation induces rapid eye movement sleep that is dependent upon the cholinergic system. Neuroscience, 156(1), 1-10. https://doi.org/10.1016/j.neuroscience.2008.06.067

McCarley, R. W., Greene, R. W., Rainnie, D., & Portas, C. M. (1995, October). Brainstem neuromodulation and REM sleep. In Seminars in Neurosciences (Vol. 7, No. 5, pp. 341-354). Philadelphia, PA, USA: Saunders Scientific Publications, c1989-c1998. https://doi.org/10.1006/smns.1995.0037

McLachlan, E. M. (1978). The statistics of transmitter release at chemical synapses. Int Rev Physiol, 17, 49-117.

Monday, H. R., Younts, T. J., & Castillo, P. E. (2018). Long-term plasticity of neurotransmitter release: emerging mechanisms and contributions to brain function and disease. Annual review of neuroscience, 41(1), 299-322. https://doi.org/10.1146/annurev-neuro-080317-062155

Niwa, Y., Kanda, G. N., Yamada, R. G., Shi, S., Sunagawa, G. A., Ukai-Tadenuma, M., ... & Ueda, H. R. (2018). Muscarinic acetylcholine receptors Chrm1 and Chrm3 are essential for REM sleep. Cell Reports, 24(9), 2231-2247. https://doi.org/10.1016/j.celrep.2018.07.082

Peever, J., & Fuller, P. M. (2017). The biology of REM sleep. Current biology, 27(22), R1237-R1248. https://doi.org/10.1016/j.cub.2017.10.026

Perrins, R., & Roberts, A. (1994). Nicotinic and muscarinic ACh receptors in rhythmically active spinal neurones in the Xenopus laevis embryo. The Journal of Physiology, 478(2), 221-228. https://doi.org/10.1113/jphysiol.1994.sp020244

Picciotto, M. R., Higley, M. J., & Mineur, Y. S. (2012). Acetylcholine as a neuromodulator: cholinergic signaling shapes nervous system function and behavior. Neuron, 76(1), 116-129. https://doi.org/10.1016/j.neuron.2012.08.036

Pino, E., Kunizawa, H., Yamuy, J., & Borde, M. (2017, July). In vitro model for the study of the role of the mesopontine region in rapid eye movement (REM) sleep and wakefulness. In Anales de la Facultad de Medicina (Vol. 4, No. 1, pp. 82-136). https://doi.org/10.25184/anfamed2017.4.1.6

Pollock, M. S., & Mistlberger, R. E. (2003). Rapid eye movement sleep induction by microinjection of the GABA-A antagonist bicuculline into the dorsal subcoeruleus area of the rat. Brain research, 962(1-2), 68-77. https://doi.org/10.1016/S0006-8993(02)03956-2

Raastad, M., Storm, J. F., & Andersen, P. (1992). Putative single quantum and single fibre excitatory postsynaptic currents show similar amplitude range and variability in rat hippocampal slices. European Journal of Neuroscience, 4(1), 113-117. https://doi.org/10.1111/j.1460-9568.1992.tb00114.x

Regehr, W. G. (2012). Short-term presynaptic plasticity. Cold Spring Harbor perspectives in biology, 4(7), a005702. https://doi.org/10.1101/cshperspect.a005702

Reinoso-Suárez, F., de la Roza, C., Rodrigo-Angulo, M. L., de Andrés, I., Núñez, Á., & Garzón, M. (2010). GABAergic Mechanisms in the Ventral Oral Pontine Tegmentum: The REM Sleep-Induction Site-in the Modulation of Sleep-Wake States. GABA and Sleep: Molecular, Functional and Clinical Aspects, 233-252. https://doi.org/10.1007/978-3-0346-0226-6_11

Rose, H. J., & Metherate, R. (2005). Auditory thalamocortical transmission is reliable and temporally precise. Journal of neurophysiology, 94(3), 2019-2030. https://doi.org/10.1152/jn.00860.2004

Rozov, A., & Burnashev, N. (1999). Polyamine-dependent facilitation of postsynaptic AMPA receptors counteracts paired-pulse depression. Nature, 401(6753), 594-598. https://doi.org/10.1038/44151

Sanford, L. D., Tang, X., Xiao, J., Ross, R. J., & Morrison, A. R. (2003). GABAergic regulation of REM sleep in reticularis pontis oralis and caudalis in rats. Journal of neurophysiology, 90(2), 938-945. https://doi.org/10.1152/jn.00993.2002

Saper, C. B., & Fuller, P. M. (2017). Wake-sleep circuitry: an overview. Current opinion in neurobiology, 44, 186-192. https://doi.org/10.1016/j.conb.2017.03.021

Sapin, E., Lapray, D., Bérod, A., Goutagny, R., Léger, L., Ravassard, P., ... & Luppi, P. H. (2009). Localization of the brainstem GABAergic neurons controlling paradoxical (REM) sleep. PloS one, 4(1), e4272. https://doi.org/10.1371/journal.pone.0004272

Sastre, J. P., Buda, C., Kitahama, K., & Jouvet, M. (1996). Importance of the ventrolateral region of the periaqueductal gray and adjacent tegmentum in the control of paradoxical sleep as studied by muscimol microinjections in the cat. Neuroscience, 74(2), 415-426. https://doi.org/10.1016/0306-4522(96)00190-X

Scammell, T. E., Arrigoni, E., & Lipton, J. O. (2017). Neural circuitry of wakefulness and sleep. Neuron, 93(4), 747-765. https://doi.org/10.1016/j.neuron.2017.01.014

Semba, K. (1993). Aminergic and cholinergic afferents to REM sleep induction regions of the pontine reticular formation in the rat. Journal of Comparative Neurology, 330(4), 543-556. https://doi.org/10.1002/cne.903300410

Silver, R. A., Momiyama, A., & Cull-Candy, S. G. (1998). Locus of frequency-dependent depression identified with multiple-probability fluctuation analysis at rat climbing fibre-Purkinje cell synapses. The Journal of physiology, 510(3), 881-902. https://doi.org/10.1111/j.1469-7793.1998.881bj.x

Stevens, D. R., Birnstiel, S., Gerber, U., McCarley, R. W., & Greene, R. W. (1993). Nicotinic depolarizations of rat medial pontine reticular formation neurons studied in vitro. Neuroscience, 57(2), 419-424. https://doi.org/10.1016/0306-4522(93)90073-O

Vanini, G., Torterolo, P., McGregor, R., Chase, M. H., & Morales, F. R. (2007). GABAergic processes in the mesencephalic tegmentum modulate the occurrence of active (rapid eye movement) sleep in guinea pigs. Neuroscience, 145(3), 1157-1167. https://doi.org/10.1016/j.neuroscience.2006.12.051

Vanini, G., Wathen, B. L., Lydic, R., & Baghdoyan, H. A. (2011). Endogenous GABA levels in the pontine reticular formation are greater during wakefulness than during rapid eye movement sleep. Journal of Neuroscience, 31(7), 2649-2656. https://doi.org/10.1523/JNEUROSCI.5674-10.2011

Vanini, G., Lydic, R., & Baghdoyan, H. A. (2012). GABA-to-ACh ratio in basal forebrain and cerebral cortex varies significantly during sleep. Sleep, 35(10), 1325-1334. https://doi.org/10.5665/sleep.2106

Vazquez, J., & Baghdoyan, H. A. (2004). GABAA receptors inhibit acetylcholine release in cat pontine reticular formation: implications for REM sleep regulation. Journal of neurophysiology, 92(4), 2198-2206. https://doi.org/10.1152/jn.00099.2004

Wang, Y. Q., Liu, W. Y., Li, L., Qu, W. M., & Huang, Z. L. (2021). Neural circuitry underlying REM sleep: A review of the literature and current concepts. Progress in Neurobiology, 204, 102106. https://doi.org/10.1016/j.pneurobio.2021.102106

Watson, C. J., Lydic, R., & Baghdoyan, H. A. (2011). Sleep duration varies as a function of glutamate and GABA in rat pontine reticular formation. Journal of neurochemistry, 118(4), 571-580. https://doi.org/10.1111/j.1471-4159.2011.07350.x

Weber, F., & Dan, Y. (2016). Circuit-based interrogation of sleep control. Nature, 538(7623), 51-59. https://doi.org/10.1038/nature19773

Weber, F., Chung, S., Beier, K. T., Xu, M., Luo, L., & Dan, Y. (2015). Control of REM sleep by ventral medulla GABAergic neurons. Nature, 526(7573), 435-438. https://doi.org/10.1038/nature14979

Weber, F., Hoang Do, J. P., Chung, S., Beier, K. T., Bikov, M., Saffari Doost, M., & Dan, Y. (2018). Regulation of REM and non-REM sleep by periaqueductal GABAergic neurons. Nature communications, 9(1), 354. https://doi.org/10.1038/s41467-017-02765-w

Weber, F. (2017). Modeling the mammalian sleep cycle. Current opinion in neurobiology, 46, 68-75. https://doi.org/10.1016/j.conb.2017.07.009

Wonnacott, S. (1997). Presynaptic nicotinic ACh receptors. Trends in neurosciences, 20(2), 92-98. https://doi.org/10.1016/S0166-2236(96)10073-4

Xi, M. C., Morales, F. R., & Chase, M. H. (1999). Evidence that wakefulness and REM sleep are controlled by a GABAergic pontine mechanism. Journal of neurophysiology, 82(4), 2015-2019. https://doi.org/10.1152/jn.1999.82.4.2015

Xi, M. C., Morales, F. R., & Chase, M. H. (2001). Induction of wakefulness and inhibition of active (REM) sleep by GABAergic processes in the nucleus pontis oralis. Archives italiennes de biologie, 139(1-2), 125-145.

Xi, M. C., Morales, F. R., & Chase, M. H. (2004). Interactions between GABAergic and cholinergic processes in the nucleus pontis oralis: neuronal mechanisms controlling active (rapid eye movement) sleep and wakefulness. Journal of Neuroscience, 24(47), 10670-10678. https://doi.org/10.1523/JNEUROSCI.1987-04.2004

Yamasaki, M., Matsui, M., & Watanabe, M. (2010). Preferential localization of muscarinic M1 receptor on dendritic shaft and spine of cortical pyramidal cells and its anatomical evidence for volume transmission. Journal of Neuroscience, 30(12), 4408-4418. https://doi.org/10.1523/JNEUROSCI.5719-09.2010

Zhang, L., & Warren, R. A. (2002). Muscarinic and nicotinic presynaptic modulation of EPSCs in the nucleus accumbens during postnatal development. Journal of neurophysiology, 88(6), 3315-3330. https://doi.org/10.1152/jn.01025.2001

Zoli, M., Pucci, S., Vilella, A., & Gotti, C. (2018). Neuronal and extraneuronal nicotinic acetylcholine receptors. Current neuropharmacology, 16(4), 338-349. https://doi.org/10.2174/1570159X15666170912110450

FIGURE LEGENDS

Figure 1. Main functional features of evoked inhibitory postsynaptic currents (eIPSCs). A. **Left:** Representative eIPSCs recorded at holding potentials (V_{hold}) ranging from -70 to +70 mV, in 20 mV increments. **Right:** current-voltage relationship (N=3) with the best-fit non-linear regression: $y = -4.9842 + 0.7268x$, $r^2 = 0.8692$. **B. Top, left:** cell-attached recordings from a PnO neuron after replacing standard ACSF with 9 mM KCl-ACSF (see *Methods*). Inset: experimental protocol. **Top, right:** example extracellular spike from the same recording, with individual raw traces (gray) superimposed and the average trace shown in black. Bottom: raster plot of 10 consecutive trials, aligned at t=-6.05 s before 1 mM GABA injection (arrowheads mark injection times; shaded area corresponds to the raw trace above). **C. Left**: whole-cell recordings of IPSCs evoked by paired-pulse stimulation in a representative experiment (V_{hold} = -70 mV). Raw data from 20 trials are shown in gray, with their average in black. Inset: stimulation protocol. Oblique arrows indicate traces representing failures (i.e., no responses). **Right:** Scatter plot of R_1 peak amplitudes and paired-pulse ratios (PPRs) from 51 observations. Bars are the mean ± SD **D.** Plot of PPR versus $1/CV^2$ for R_1. Non-linear regression yielded the best-fit curve described by: $y = 0.8939 + 0.7136/x$ (N = 51, $R^2 = 0.5271$).

Figure 2. Short-term plasticity profile of activated GABAergic synapses during short-train stimulation. A. Left: representative whole-cell recordings of IPSCs evoked by a train of 5-pulses/15 Hz delivered in the LDT/PPT at a V_{hold} = -70 mV. Gray traces show 20 individual trials, and the black trace depicts their average. Inset: stimulation protocol. **Right:** Scatter plot of R1 peak amplitudes and short-term plasticity ratios (STPRs). Each dot represents the mean value for a single experiment, while the bars indicate the mean ± SD. **B.** Plot of STPR versus $1/CV^2$ for R1. A non-linear regression best-fit yielded the equation: $y = 0.8679 + 1.0059/x$ (N = 57, $R^2 = 0.4032$). Discontinuous lines mark the 95% prediction band. **C.** Scatter plot of $1/CV^2$ (R_1) and of R_1 peak amplitudes pooled from both paired-pulse and short-train stimulation experiments (N = 108). Data are sorted according to the paired-pulse ratio (PPR) into two groups: short-term depression (STD; PPR < 1) and short-term facilitation (STF; PPR > 1). Bars depict the mean ± SD. *Mann-Whitney rank sum test: STD: N=29; STF: N=79; ***p<0.001; n.s.: not significant*. **D. Left:** Normalized peak amplitudes for pulses R1–R5 (values normalized to R1). The thick line represents the average profile. **Right:** Plot of STPR versus

PPR for all experiments (N = 57); the shaded area indicates the region corresponding to short-term facilitation (STF; PPR > 1 and STPR > 1).

Figure 3. Modulation of activated GABAergic synapses by *carbachol* (CCh). A. Synaptic depression. A1. Top: whole-cell recordings of eIPSCs obtained before (control, Ctrl.) and after the injection of 1 mM carbachol (CCh.); the washout is also shown (wo). **Bottom**: mean amplitude of R_1 before (Ctrl.) and following CCh microinjections. Bars represent the median ± the interquartile range. **A2**. PPR values sorted according to whether CCh induced an increase or a decrease relative to control. **B. Synaptic facilitation.** Same as A but illustrating CCh-induced increases of R1 mean amplitude (**B1**) and the corresponding changes in the PPR (**B2**). *Wilcoxon signed-rank test: * p<0.05, ** p<0.01, *** p<0.001, n.s.: not significant.* Sample size (N) is indicated for each graph. Shaded areas in A2 and B2 highlight the effects of CCh on PPR, consistent with presynaptic inhibition (A2) and presynaptic facilitation (B2); see main text for details.

Figure 4. Modulation of activated GABAergic synapses by *muscarine* and *nicotine*. A. Modulation of synaptic efficacy and short-term plasticity by muscarine. **A1**. Top: Representative eIPSCs recorded before (Ctrl.) and immediately following juxtacellular injection of muscarine (Musc., 50-150 ms/20-30 psi, 10 μM); wo: washout. Bottom: $R_{1(avg)}$ before (Ctrl.) and following the muscarine injection (Musc). **A2.** PPRs (left), STPRs (middle) and Q_{inh} (right) before (Ctrl.) and after muscarine injection (Musc.). **B.** Same as A but showing effects of nicotine (50-150 ms/20-30 psi, 20 μM). R_1, PPR, STPR: *Wilcoxon signed-rank test, *** p<0.01;* Q_{inh}: *paired t-test: * p<0.05, ** p<0.01; n.s: not significant;* Sample size (N) is indicated for each graph. Bars indicate the median ± the interquartile range.

Figure S1. Effects of GABAB-receptor activation on GABAergic synaptic inputs to PnO neurons. A. R_1 peak amplitudes (left) and PPRs (right) before (Ctrl.) and immediately following juxtacellular injection of 100 μM baclofen (50-150 ms/20-30 psi, Bac.); paired t-test: N=9, n.s.: not significant. *Bars are the median ± the interquartile interval*. **B**. Cumulative probability distribution of amplitude of sIPSCs sampled during a representative experiment illustrated in **A**; Plots were constructed by detecting consecutive events during 60-120 s gap-free recordings sampled before (Ctrl.), immediately following (Bac.) and 15 min after (wo: washout) baclofen injection. Immediately after Baclofen injection, the cumulative probability distribution shifted leftward compared to control

(*Kolmogorov–Smirnov test: ** p<0.005*) indicative of a reduction in event amplitude with a suppression of larger events.

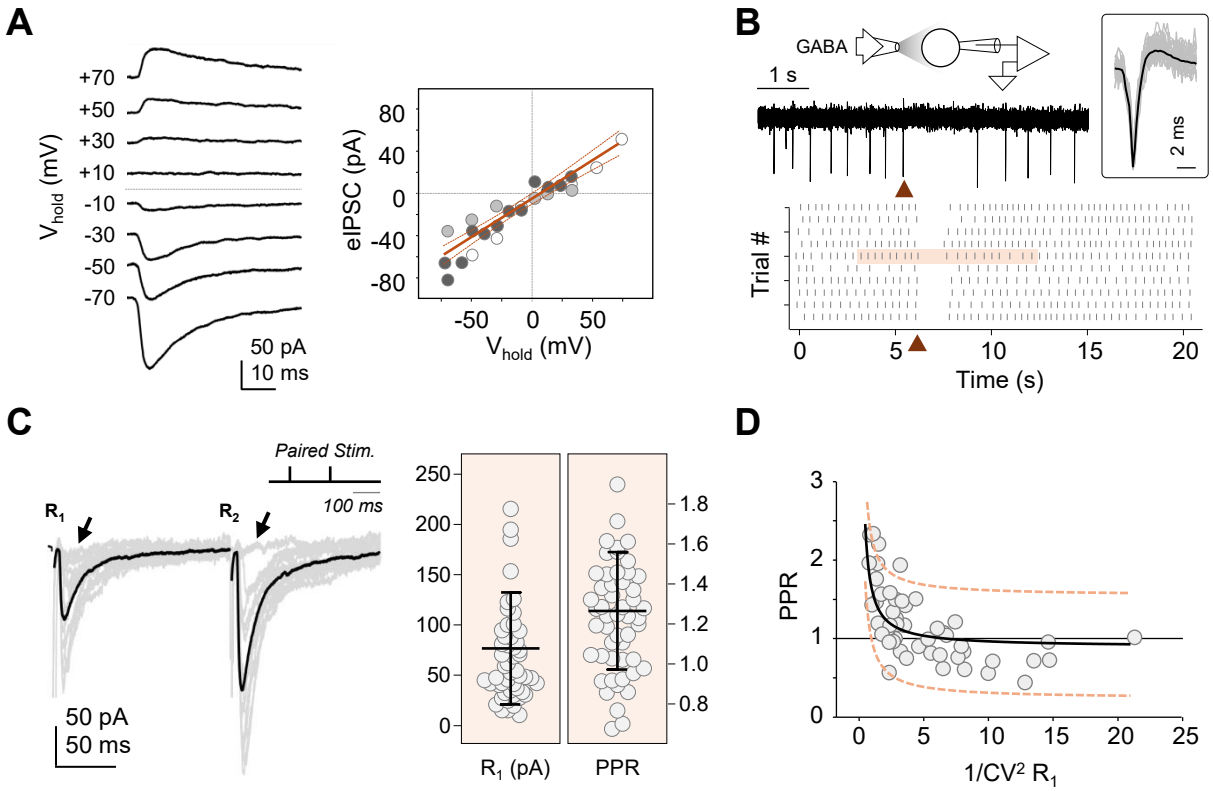

Fig. 1 Pino et al.

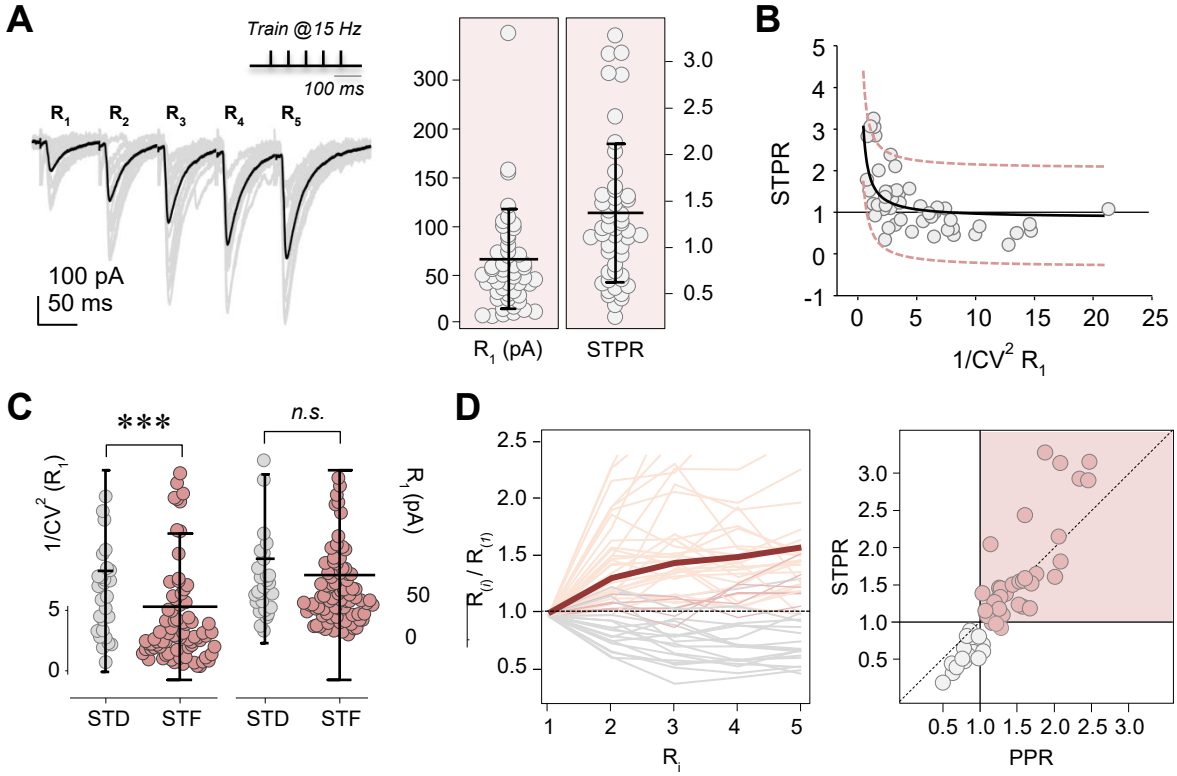

Fig. 2 Pino et al.

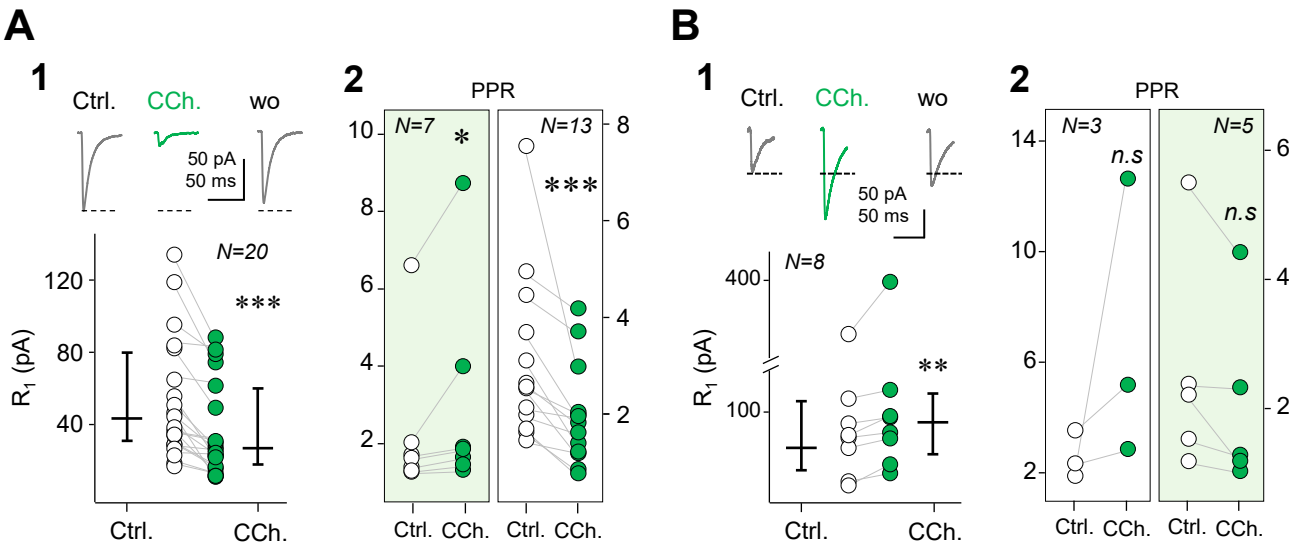

Fig. 3 Pino et al.

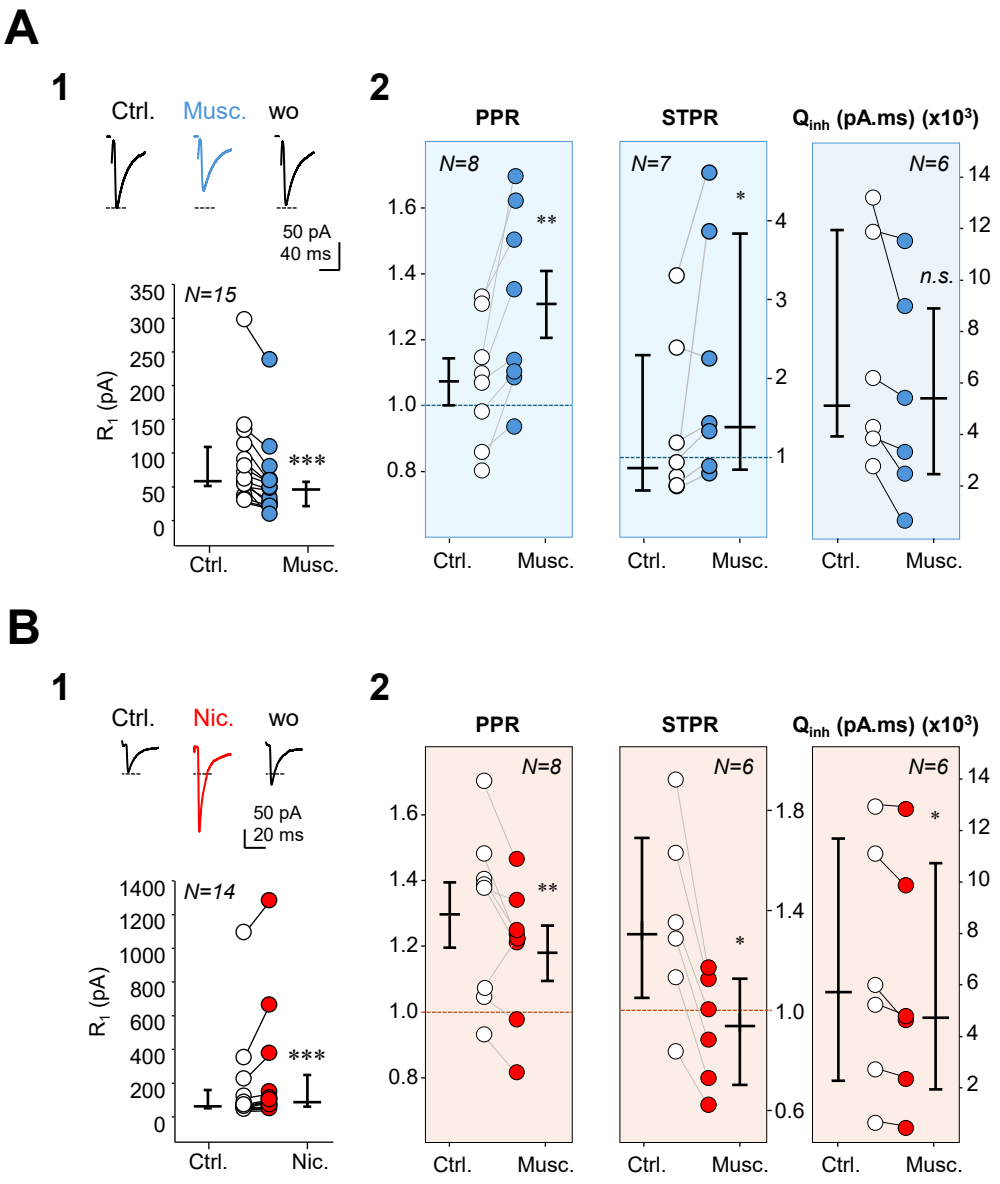

Fig. 4 Pino et al.

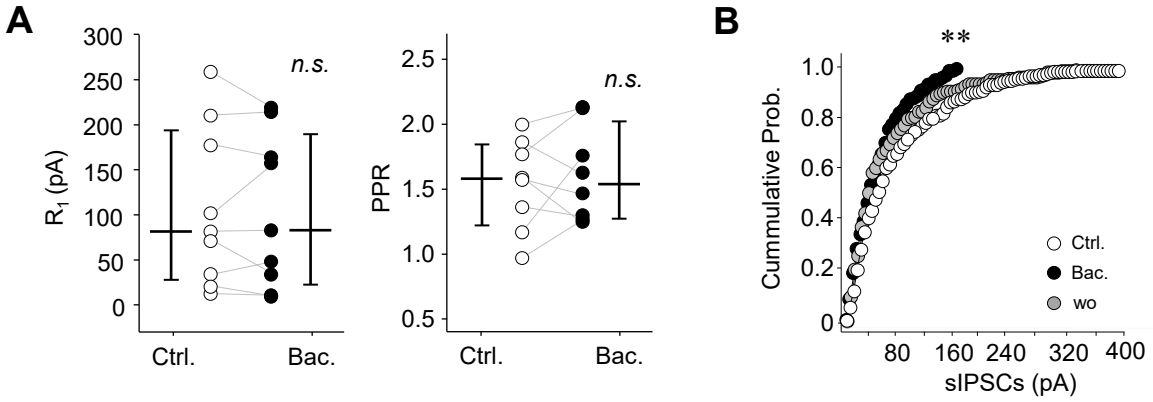

Fig. S1 Pino et al.